

Differential impacts of the head on *Platynereis dumerilii* peripheral circadian rhythms

Enrique Arboleda^{1,3}, Martin Zurl^{1,2} and Kristin Tessmar-Raible^{1,2*}

¹ Max F. Perutz Laboratories, University of Vienna, Vienna BioCenter, Dr. Bohr-Gasse 9/4, A-1030 Vienna

² Research Platform “Rhythms of Life”, University of Vienna, Vienna BioCenter, Dr. Bohr-Gasse 9/4, A-1030 Vienna

³Current address: Institut de Génomique Fonctionnelle de Lyon (IGFL), École Normale Supérieure de Lyon, 32 avenue Tony Garnier, 69007 Lyon, France

* Corresponding Author: kristin.tessmar@mfpl.ac.at

Abstract

Background: The marine bristle worm *Platynereis dumerilii* is a useful functional model system for the study of the circadian clock and its interplay with others, e.g. circalunar clocks. The focus has so far been on the worm’s head. However, behavioral and physiological cycles in other animals typically arise from the coordination of circadian clocks located in the brain and in peripheral tissues. Here we focus on peripheral circadian rhythms and clocks, revisit and expand classical circadian work on the worm’s chromatophores, investigate locomotion as read-out and include molecular analyses.

Results: We establish that different pieces of the trunk exhibit synchronized, robust oscillations of core circadian clock genes. These circadian core clock transcripts are under strong control of the light-dark cycle, quickly losing synchronized oscillation under constant darkness, irrespective of the absence or presence of heads. Different wavelengths are differently effective in controlling the peripheral molecular synchronization. We have previously shown that locomotor activity is under circadian clock control. Here we show that upon decapitation it still follows the light-dark cycle, but does not free-run under constant darkness. We also observe the rhythmicity of pigments in the worm’s individual chromatophores, confirming that chromatophore size

23 changes follow a circadian pattern. These size changes continue under constant darkness, but cannot be re-
24 entrained by light upon decapitation.

25 **Conclusions:** Here we provide the first basic characterization of the peripheral circadian clock of *Platynereis*
26 *dumerilii*. In the absence of the head, light is essential as a major synchronization cue for peripheral molecular
27 and locomotor circadian rhythms. Circadian changes in chromatophore size can however continue for several
28 days in the absence of light/dark changes and the head. Thus, the dependence on the head depends on the
29 type of peripheral rhythm studied. These data show that peripheral circadian rhythms and clocks should be
30 considered when investigating the interactions of clocks with different period lengths, a notion likely also true
31 for other organisms with circadian and non-circadian clocks.

32 **Keywords:** marine, annelid, daily, rhythm, clock, chromatophores, transcription, locomotion

33 **Introduction**

34 Extensive research focusing on drosophilids and mice showed that the daily behavioral, physiological and
35 metabolic cycles in animals arise from coordination of central circadian clocks located in the brain and
36 peripheral clocks present in multiple tissues (1–3). In *Drosophila*, several peripheral tissues and appendages
37 (e.g. Malpighian tubules, fat bodies and antennae) have autonomous peripheral clocks that are directly
38 entrained by environmental cycles independent of the central clock, while others, such as oenocytes, are
39 regulated by the circadian clock located in the brain (4,5). The mammalian circadian system is highly
40 hierarchically organized. The master central clock in the suprachiasmatic nucleus (SCN) of the brain (often
41 referred to as a “conductor”) synchronizes internal clock timing to the environmental solar day by passing the
42 information to the peripheral clocks via endocrine and systemic cues (6,7). These peripheral clocks also have
43 self-sustained circadian oscillators, with the master clock coordinating their phase to prevent
44 desynchronization among peripheral tissues, rather than acting as a pacemaker responsible for the periodicity
45 of the cycling itself (8). Besides being phase-controlled by the “SCN conductor”, several mammalian peripheral

clocks (e.g. in liver and kidney) have been shown to directly respond to non-photic entrainment cues, like food or exercise (9).

For marine organisms, biorhythms of various period lengths, including circadian and circalunar, have been described across phyla, e.g. as changes in activity levels, coloration and reproductive cycles (reviewed in 10–13). Where studied in detail, like in the marine bristle worm *Platynereis dumerilii* and the marine midge *Clunio marinus*, the light of sun and moon are known to serve as major entrainment cues (14–16). Over recent years, marine rhythms and their possible underlying clockworks have been receiving increasing attention, as the interplay of clocks and rhythms of different organisms is a crucial aspect for ecology (17).

Molecular data on rhythms and clocks in marine invertebrates have become increasingly available over the last decade, now including the bivalves *Mytilus californianus* (18) and *Crassostrea gigas* (19), the sea slugs *Hermisenda crassicornis*, *Melibe leonina* and *Tritonia diomedea* (20,21), the isopod *Eurydice pulchra* (22–24), the amphipod *Talitrus saltator* (25), the lobsters *Nephrops norvegicus* (26) and *Homarus americanus* (27), the mangrove cricket *Apteronomobius asahinai* (28), the copepods *Calanus finmarchicus* (29) and *Tigriopus californicus* (30), the Antarctic krill *Euphausia superba* (31–34), the Northern krill *Meganyctiphanes norvegica* (27), the marine midge *Clunio marinus* (15,35), and the marine polychaete *Platynereis dumerilii* (14,36). On the marine vertebrate side, especially teleost fish species have been investigated (37–45).

While most of the above mentioned species are difficult to maintain in the laboratory and to investigate at the level of molecular genetics, *P. dumerilii* is a particularly well-established laboratory model (46,47) for marine chronobiological research. It possesses interacting circadian and circalunar clocks and, complementing the molecular work, a detailed analysis of its circadian locomotor activities has been described for adult stages (14,16,48). Evidence of circadian activity also exists for young larval stages within the first days of their development (49). Similar to the isopod *E. pulchra* (22,23), *P. dumerilii* also exhibits a circadian rhythm in its body pigmentation (50–52). This rhythm in pigment cell extension versus contraction was described as a segment-autonomous process (50–52), indicating the presence of autonomous peripheral circadian oscillators.

70 As *P. dumerilii* beheaded individuals survive well for up to two weeks (53), this feature can be used to study
 71 living animals in the absence of its circadian brain clocks. Moreover, *P. dumerilii* has primitive morphological
 72 and genetic features, and is hence viewed as evolutionarily slowly evolving (54), a feature which is particularly
 73 interesting for understanding the ancestral features of different clocks and rhythms, as well as in the light of
 74 the- certainly debated hypothesis- that vertebrates originated from a polychaete-like animal (11).

75 The work presented here is the first detailed characterization of *P. dumerilii* peripheral circadian rhythms and
 76 clocks, covering analyses of transcript level changes of core circadian clock genes, as well as body pigmentation
 77 and locomotor activity.

78 Results

79 ***Platynereis dumerilii* peripheral circadian clock gene transcripts quickly desynchronize under complete** 80 **darkness**

81 As a starting point, we aimed to test for the presence of peripheral clocks in the body of *P. dumerilii* adults.
 82 Based on the previously described and tested molecular components of the core circadian oscillator in *P.*
 83 *dumerilii* heads (14), we analyzed the daily transcriptional fluctuation of *bmal*, *period* and *tr-cry* as
 84 representative components of the circadian clock by RT-qPCR (Fig. 1). Daily fluctuation of *bmal*, *period*, *tr-cry*,
 85 *timeless*, *clock* and *pdp1* transcripts in the trunk are overall similar to those in the head (Fig. 1A,B, for *timeless*,
 86 *clock* and *pdp1* see Additional file 1: Figure S1 A-C, compare also with (14)). Results were similar irrespective
 87 of the segment positions used for analyses, *i.e.* whole trunk (Fig.1), last 5-7 segments of the body or the
 88 adjacent 5-7 segments towards the anterior part of the animal (Additional file 1: Figure S1 D-F) produced
 89 consistent results. *Pdu-tr-cry* appears to be the gene that deviates most in this comparison. We attribute this
 90 difference to a higher variability of the transcript level synchronization in the trunk given that in most cases it
 91 corresponds to the oscillations observed in the head (compare Fig.1, 2A, 3C, Additional file 1: Figure S1 A-C,
 92 and (14)).

We next tested if the peripheral circadian clock transcript oscillations would continue synchronously under constant darkness for three days. All tested transcripts dampened strongly, with *tr-cry* still exhibiting weak oscillations (Fig.1C).

Light signals are sufficient to maintain circadian clock transcripts in the trunk, independent of the head

To analyze if the peripheral circadian clock transcript oscillations in the worm's body were dependent on the circadian clock in its head, we took advantage of the fact that bodies of decapitated animals survive in seawater for two weeks (53). Adult animals were decapitated and placed under standard light-dark cycles for three days before RNA extraction. Relative transcript levels of *bmal*, *period* and *tr-cry* exhibited overall similar levels and continued a clear diel cycling of expression in trunks of decapitated animals (Fig. 2A), indicating that the peripheral circadian clock gene expression continues to synchronously run even in the absence of the brain circadian clock. When we tested core circadian clock transcript oscillations in trunks of decapitated animals under three days of constant darkness, no significant oscillations were detectable (Fig. 2B).

By placing decapitated animals on an inverted light cycle, we next tested for the capacity of peripheral clocks to be re-synchronized by light, again using the transcript oscillations of *bmal*, *per* and *tr-cry* as readout. Cycling of *bmal* and *per* was re-entrained to the inverted cycle when exposed to white, red or blue light (Fig. 3A,B, for spectra and intensity see in Additional file 2: Figure S2). *tr-cry* transcript oscillations differed from this, in that white and blue light could re-entrain its peripheral oscillations as in the case of *bmal* and *per*, whereas red light did not (Fig. 3C). Overall, these results demonstrate that the peripheral circadian clock transcripts directly respond to changes in the light cycle, independent of the head.

Chromatophore size follows a circadian pattern and free-runs under constant darkness

In order to assess how our findings on core circadian clock transcripts oscillations might relate to physiology and behavior, we investigated possible outputs of peripheral circadian clocks, starting with changes in chromatophore size in the trunk. Chromatophores are located along the dorsal part of the segmented body of *P. dumerilii*. Based on light microscopy analyses it had previously been shown that the worm's

117 chromatophores exhibit a segment-autonomous, diel contraction-expansion rhythm with increasing size
118 during the day and decreasing size at night (50–52).

119 We first aimed at identifying a possibility to automatize the recording of chromatophore changes. We found
120 that chromatophores exhibit a well-detectable autofluorescence under 488 nm light (Fig. 4A,B), which can be
121 used for automatic detection by any image software. In order to characterize the pattern of
122 contraction/expansion of the chromatophores, animals were photographed every three hours over the course
123 of 24h using a fluorescence microscope. We found a clear circadian pattern with higher chromatophore
124 expansion between ZT2 and ZT11 (Fig. 4C), and a sharp drop on chromatophore size from ZT11 to ZT14, before
125 lights go off and the subjective night period starts, already suggestive of an autonomous clock-driven process
126 and not a direct light response, again consistent with previous observations (55).

127 We next focused on sampling points corresponding to ZT/CT2 and ZT/CT14, during which a ~60% drop in
128 chromatophore size was evident (Fig. 4C, Fig. 5A,B), and used these two time points as a reference for the
129 study of circadian cycling of pigmentation over multiple days. Chromatophores expansion/contraction
130 continued to cycle in animals placed under constant darkness for five consecutive days (Fig. 5C)

131 For evidence that the light used for measuring chromatophore size is not causing re-entrainment in this case,
132 see below.

133 **Circadian pattern of chromatophore size free-runs, but cannot be re-entrained by light in decapitated** 134 **animals**

135 In order to assess if the regulation of the cycling on chromatophore size is governed by peripheral clocks,
136 decapitated animals were used. The same animals were photographed at ZT2 and ZT14 prior to decapitation
137 as a starting reference point. Following decapitation, worms were placed in constant darkness for four days,
138 and subsequently exposed again to a normal LD cycle for additional three days. Chromatophores sizes were
139 registered along the experiment from day 0 to day 4, and again on day 7 to test for possible re-entrainment.
140 Upon decapitation, animals under DD conditions initially continue to exhibit clear rhythms of chromatophore

size changes (Fig. 5D, for individual replicas see Additional file 3: Figure S3). Starting with the second day in DD, the rhythm will however start to dampen and become statistically non-significant by day 3 (Fig.5D). Subsequent exposure to a normal LD cycle did not lead to a re-synchronization of the chromatophore rhythm (Fig. 5D). Consistently, cycling of chromatophore size does not get re-entrained on decapitated animals under an inverted LD cycle applied for 5 days (Fig. 5E).

In order to rule out that we may have missed phase-shifts on decapitated animals due to the exposure to the 488nm light during the measurement procedure (due to too low sampling frequency), we also performed a more densely spaced 24-hour sampling on day 5 in LD (post decapitation). This experiment confirmed our interpretation of a dampening of the chromatophore size rhythm and inability to re-entrain in the absence of the head (Fig. 5F). All together, these results suggest a circadian pattern of chromatophore size governed by a peripheral clock, which however requires the head to maintain extended synchronization and for re-entrainment by light.

Circadian locomotor activity follows the light-dark cycle, but does not free-run under constant darkness in decapitated worms

We next turned to locomotor activity as a read-out for circadian clock activity. We have previously shown that *P. dumerilii* during new moon (circalunar phase of its circalunar clock) exhibits nocturnal circadian locomotor activity, which free-runs under constant darkness for at least three days (14,48). We meanwhile established an automated worm locomotor behavioral tracking system, which measures worm activity as distance moved of the worm's center point within 6 min time bins (56–58). It should be noted that this new type of analysis measures relative distance moved, compared to the binary (movement: yes or no) manual scoring done by Zantke et al. (14). Intact worms showed a significant circadian rhythmic locomotor activity under LD and DD conditions (Fig. 6A,B, for individual actograms see Additional file 4: Figure S4). In contrast decapitated worms exhibit an overall severe reduction in movement and rhythmicity (Fig.6C,D, for individual actograms see Additional file 5: Figure S5). No significant circadian rhythmicity can be observed under constant darkness in

headless worms (Fig.6C,D), with one exception. Overall, these data suggest that lack of signals from the brain lead to a general suppression of movement and lack of circadian information for the locomotor output. Headless worms are not generally paralyzed, as they can show spontaneous bursts of movement (Additional file 5: Figure S5) and- depending on their stage at decapitation- can proceed to maturation and the associated behavioral changes (59). Similar to the rhythmic transcript oscillations of the core circadian clock genes in the trunk, acute light functions as a synchronization cue to the periphery of headless worms, but without head or light stimuli a circadian locomotor pattern cannot be maintained by the trunk alone in 97% of the worms analyzed.

Discussion

Molecular peripheral clock

Here we examine peripheral circadian clock transcript changes and diel rhythms in chromatophore size and locomotor behavior in *P. dumerilii* in the absence and presence of its head. An endogenous circadian rhythm driving body pigmentation change in *P. dumerilii* had been previously proposed based on photographic recordings of isolated groups of body segments during the middle of the day and the night (51,52). With the exception of gills in oysters (60), there is no information on fluctuation of circadian clock genes on peripheral tissues or appendages in marine organisms. We document the expression of core circadian clock genes in the periphery of *P. dumerilii*, arguing in favor of a functional circadian peripheral clock and opening an avenue to study the molecular mechanisms of peripheral clocks in marine invertebrates. We show that light/dark cycles can (at least in part) substitute for the head as major synchronizer for continuous peripheral core circadian clock transcript oscillations. We confirm previous work on chromatophore rhythms, which - in contrast to locomotion and transcript oscillations- exhibit free-running rhythms in trunks of headless worms.

As previously reported for the central clock (14), *period* and *bmal* transcripts cycle in antiphase from each other, while *tr-cry* transcripts are neither directly in-phase nor in anti-phase with any of them. Our results on trunks show that cycling of *bmal* and *period* continues under LD conditions, but not under DD independently

189 of the head being present or absent, and can be entrained to an inverted LD cycle on decapitated animals.

190 These results suggest that the peripheral clocks are light dependent (through a yet to be identified set of

191 photoreceptors in the trunk) and get out of synchrony in the different peripheral cells and tissues on the

192 transcriptional level (at least as fast as three days in DD) in the absence of the head. A system with peripheral

193 clocks independent from the central circadian clocks in the brain and entrained directly by environmental

194 signals is reminiscent of *Drosophila melanogaster* (5). In that sense the peripheral clock in *P. dumerilii*

195 resembles that of insects, and light reception in the trunk likely occurs via Cryptochromes and/or Opsins.

196 Candidates include Go-Op sin1 and rOp sin1 (56,61).

197 Light exhibits different effects on the different readouts. In the cases of transcript oscillations and locomotor

198 activity the head is not required for its impact, suggesting that peripheral photoreceptors mediate this signal.

199 Interestingly, different wavelengths appear to have differential peripheral effects on transcript oscillations (red

200 light being able to re-entrain *per* and *bmal* trunk oscillations, but not *tr-cry*), which already indicates the

201 involvement of more than one photoreceptor. It will be interesting for future studies to understand why *tr-cry*

202 transcripts behave differently from *bmal* and *per* transcripts under different light conditions. These differences

203 could be the result of *tr-cry* only being expressed in a subset of tissues/cell types that do not desynchronize as

204 quickly.

205 As in the case of insects (5) and mammals (62), questions regarding how peripheral clocks are entrained and

206 the actual mechanisms that peripheral clock use to drive transcriptional changes on various tissues are still

207 questions to be answered in *P. dumerilii*, as is the case for the specific functions of the peripheral clocks.

208 It should be noted that our experiments were performed on the complete trunk (or at least several segments),

209 which also leaves open questions regarding the peripheral circadian cycling and their synchronizations in

210 specific segmentally repeated organs and tissues.

211 **Chromatophore size and the peripheral clock**

212 Daily changes in chromatophore size on *P. dumerilii* can be easily used as a visual read out of the circadian
213 clock, adding up to its locomotor activity, circalunar spawning and clock-related genes as means to study
214 chronobiology in this model system.

215 Remarkably, the first studies on the cyclic changes of body pigmentation in *P. dumerilii* date back to 1939 (55).
216 Based on this and further classical work, these changes in body pigmentation were already attributed to an
217 endogenous circadian rhythm present in each segment of the worm's body (50–52), pointing at the existence
218 of peripheral circadian clocks long before their molecular mechanism had been unraveled and circadian
219 peripheral oscillations were proven to exist in the peripheral tissues in mammals (63–66). Our analyses support
220 the classical studies on *Platynereis*, in that chromatophore size in the body of *P. dumerilii* is higher during day
221 time, with a major drop before the night begins; which argues in favor of a clock-driven manifestation and not
222 a direct light response. The average magnitude of this change corresponds with previous quantitative reports
223 by Fischer (50). We report that individuals placed in DD for five days still exhibit a significant daily difference
224 on chromatophore size, although its maximum value decreases by 25% compared to the initial LD conditions.
225 It has been reported that such cycling starts to fade on individual chromatophores after seven days in DD (50),
226 but we did not test for the long term stability of the cycle for individual chromatophores. Noticeably, a similar
227 circadian cycling of chromatophore size on DD and inverted LD cycles has been shown for the marine isopod
228 *Eurydice pulchra* (23), posing the questions if this regulation is similar.

229 Changes in chromatophore size with a circadian cycling is commonly seen in crustaceans (23,67–69). There is
230 usually an increase in size during the day thought to be related to UV protection (70), but an inverted pattern
231 of bigger chromatophore size during the night, to possibly enable individuals to camouflage with the substrate,
232 can also be found (71). The fact that *P. dumerilii* is mostly active during the night (14), when pigmentation is
233 lower, does not argue in favor of a camouflage role; especially since pigmentation does not respond to changes
234 in background brightness (50). The most parsimonious option is therefore a role of pigmentation in protecting
235 the animal from UV light. It should be noted, however, that it has also been often proposed, but not tested,
236 that circadian changes in pigmentation might be a mechanism related to energy saving (72).

Remarkably, in our hands the re-entrainment of chromatophore rhythms by light requires the presence of the head. This might be either because the required photoreceptor(s) are located in the head or because hormonal feedback signals, such as *Pdu*-PDF (pigment dispersing factor) (73), are required for the synchronization process. It is likely that pigmentation in *P. dumerilii* is controlled by a hormonal process, as in some crustaceans (68,69,74), which in turn is governed by the central clock. The hormonal nature of the cycling on chromatophore size has been further supported by the immediate reaction of chromatophores, present on isolated skin tissue, when coelomic fluid from *P. dumerilii* during a given time point (e.g. day or night) is added (52).

Finally, while we overall confirm previous work on the chromatophore rhythms in the trunk of *P. dumerilii*, there is one clear difference between our findings and that of Röseler (52). Her work shows that chromatophore rhythms can still be re-entrained by white light even in the absence of the prostomium (head), whereas in our hands decapitated animals do not re-entrain their chromatophore rhythm in response to white light. We identified two main reasons that might explain this discrepancy. The materials and methods of her paper do not state the light intensity and spectrum. It is thus possible that this strongly deviates from our conditions. The other difference is the extent of head removal. In our study we removed the head including the jaw piece, whereas Röseler (52) specifies prostomium-removal, which implies that her worms still possessed the jaw and the surrounding tissue. This region possesses multiple neurons and neurosecretory cells, which could be important for proper re-entrainment. Further work will certainly help to disentangle these differences.

Conclusions

We find that the overall circadian clock transcript oscillations of the trunk are under strong control of the light-dark cycle and do not show synchronized oscillation under constant darkness, irrespective of the absence or presence of heads. In the absence of heads, locomotor activity is also strongly coordinated by the light-dark cycle. In contrast, circadian changes of body pigmentation in the trunk free-run over several days in constant

261 darkness, even in the absence of the head. Jointly these data indicate that autonomous peripheral clocks exist
262 in the trunk of the bristle worm, coordinating for instance pigmentation. However, the synchronization of
263 rhythmic circadian oscillations in other peripheral tissues and their respective output are more strongly
264 coordinated by light than by the circadian oscillator positioned in the head of the worm. Our data build a basis
265 for future analyses of the multiple clocks of the bristle worm, but also suggest that peripheral clocks should be
266 taken into consideration when studying other organisms with circadian and non-circadian oscillators.

267 **Materials and Methods**

268 **Animal cultures**

269 Animals were maintained on controlled temperature and 16:8 hours light-dark (LD) or dark-dark (DD) cycle as
270 previously described (36). Sampling points are presented either as Zeitgeber Time (ZT) for light-dark conditions
271 (LD) or circadian time (CT) for constant darkness (DD).

272 **Worm decapitation**

273 Animals were anesthetized by adding a few drops of 1M MgCl₂ in the seawater until they stopped moving.
274 They were carefully placed on a microscope slide under a binocular dissecting microscope, decapitated, and
275 transferred to fresh seawater again. Decapitation was done with sterile surgical blades cutting on the first
276 segments below the pharyngeal region in order to collect only the posterior part of the body (*i.e.* the trunk).
277 They were consistently performed between ZT 13.5 and ZT14. For head samples, the region containing the
278 pharynx and the posterior end of the head was removed (see (14)).

279 **Circadian re-entrainment under white, blue and red light conditions**

280 When testing for circadian re-entrainment (*i.e.* an inverted light cycle) under white, blue or red light, animals
281 were exposed to the new conditions for seven days before sampling. Light spectra and intensities of white,
282 blue and red LEDs (ProfiLuxSimu-L from GHL advanced technology gmbh, Germany) used for circadian re-
283 entrainment were measured using an ILT950 spectrometer (International Light Technologies Inc., Peabody,

USA). Special care was taken to account for the standard conditions where the worms were housed, *i.e.* 22cm away from light source and with a transparent plastic lid positioned between the spectrometer and the light source. Measured light intensities for white, red and blue lights were $8,2 \times 10^{13}$ photons/cm²/s, $3,8 \times 10^{13}$ photons/cm²/s and $2,4 \times 10^{13}$ photons/cm²/s, respectively (for spectra see Additional file 2: Figure S2A).

288 **Total RNA extraction and RT-qPCR**

289 Total RNA was extracted from heads or trunks (*i.e.* decapitated animals) using the RNeasy Mini Kit (QIAGEN).
290 Reverse transcription was carried out using 0.4 µg of total RNA as template (QuantiTect Reverse Transcription
291 kit, QIAGEN). RT-qPCR analyses were performed using a Step-One-Plus cycler. The expression of each test gene
292 was normalized by the amount of the internal control gene *cdc5*. The relative expression was calculated using
293 the formula $1/2^{\Delta Ct}$. Primers and PCR program used are listed in Zantke et al. (14).

294 **Chromatophore size**

295 Three consecutive segments located towards the middle of the body were selected on each animal to evaluate
296 changes in chromatophore size. In order to precisely re-identify the same segments over the course of the
297 experiments, animals were anesthetized with MgCl₂ and a parapodium, two segments away from the region
298 of interest, was removed with a sterile surgical blade. When required, one animal at a time was placed on a
299 glass cover without water and extended carefully. An epifluorescence stereoscope (Zeiss Lumar) with a 488
300 nm laser and a FITC filter was used to take pictures making sure to always use the same magnification across
301 animals and sampling points. Animals were placed again in seawater until the next sampling point. Image
302 analysis was done using Adobe Photoshop. On fluorescent images, the RGB channels red and blue were
303 lowered to zero, and the three segments of interest were extracted by erasing the unwanted area
304 (chromatophores on each segment have a specific pattern, which makes their visual identification easier). A
305 new layer was generated by using the magic wand tool to single out the bright green chromatophores from
306 the background fluorescence. Using the image's histogram, the number of colored pixels was used as a proxy
307 of chromatophore size. Animals had between 20 and 40 chromatophores along the three segments, but no

effort was done to quantify size of individual chromatophores. Instead, the sum of all the chromatophores of interest were used as chromatophore size value at each time point. Absolute pixel number was expressed as a percentage of the maximum value for each animal across all time points of the experiment (i.e. $x_i / (\text{Max}\{x_i, \dots, x_j\} * 100)$). Average among biological replica and SEM were further calculated.

Locomotor Activity Assay

Immature worms of comparable size were starved for three days before the start of the assay. After decapitation, worms were placed in individual hemispherical concave wells (diameter = 35 mm, depth = 15 mm) of a custom-made 36-well clear plastic plate (as described in (56)). Intact worms were also treated with MgCl_2 for 5min prior to locomotor recording to ensure proper comparisons to decapitated worms. Video recording of worm's behavior over several days was accomplished as described previously (14), using an infrared ($\lambda = 990 \text{ nm}$) LED array (Roschwege GmbH) illuminating the behavioral chamber and an infrared high-pass filter restricting the video camera. White light was generated by custom made LEDs (Marine Breeding Systems, St. Gallen, Switzerland) with the intensity set to $5,2 \times 10^{14} \text{ photons/cm}^2/\text{s}$ at the place where worms were housed (for light spectrum see Additional file 2: Figures S2B). Trajectories of locomotor activity of individual worms were deduced from the video recordings by an automated tracking software developed by LoopBio gmbh (57, 58). Locomotor activity trajectories reflect the distance moved of each worm's center point across 6min time bins. Activity data was plotted as double-plotted actograms using the ActogramJ plugin for Fiji (75).

Statistical Analyses

Statistical analyses were performed using either the Data Analysis plug-in in Microsoft Excel using an alpha value of 0.05 (molecular and chromatophore data) or GraphPad Prism (locomotor activity data). For changes in chromatophore size, each two-sample two-tailed student's t-Test was preceded by an F-Test to check if the variances of the two groups were equal or not. To test if transcriptional changes in gene expression over time oscillated to a statistically significant difference, fold change data was analyzed for each sampling point using

single factor ANOVA. In order to ease the logistic process of analyzing a considerable amount of data, RNA samples and chromatophore size images were not analyzed blindly but chronologically as experiments were being performed. Statistical differences in locomotor activity across treatments were estimated using repeated measures ANOVA followed by Sidak's multiple comparison test. To identify the free-running period length of intact worms under DD conditions Lomb-Scargle periodogram analysis was done using the ActogramJ plugin for Fiji (75).

Ethics approval and consent to participate: All animal work was conducted according to Austrian and European guidelines for animal research.

Consent for publication: Not applicable.

Availability of data and material: All sequence resources referred to here were already published previously and submitted to public databases. All other data that support the findings of this study are available from the corresponding author upon reasonable request.

Competing interests: The authors declare that they have no competing interests.

Funding: K.T-R. received funding for this research from the European Research Council under the European Community's Seventh Framework Programme (FP7/2007–2013) ERC Grant Agreement 337011, the research platform 'Rhythms of Life' of the University of Vienna, the Austrian Science Fund (FWF, <http://www.fwf.ac.at/en/>): START award (#AY0041321) and research project grant (#P28970). M.Z. has in part been financially supported by an FWF grant to the F. Raible lab (#I2972).

None of the funding bodies was involved in the design of the study, the collection, analysis, and interpretation of data or in writing the manuscript.

Authors' contributions: EA and KTR designed the study and wrote the manuscript. MZ reviewed and commented on manuscript. EA and MZ performed experiments: MZ – locomotor activity experiments and

354 measurement of light spectra and intensities, EA – all other experiments. EA, KT and MZ did data analysis,
355 interpretation and discussion.

356 **Acknowledgements:** We thank the members of the Tessmar-Raible and Raible groups for discussions,
357 especially Juliane Zantke, Vinoth Babu Veedin Rajan, Birgit Pöhn and Max Hofbauer for sharing details on the
358 automated locomotor behavioral tracking prior to publication. Andreij Belokurov and Margaryta Borysova for
359 excellent worm care at the MFPL aquatic facility and Claudia Lohs and Katharina Schipany for excellent
360 technical assistance.

361 References

- 362 1. Mure LS, Le HD, Benegiamo G, Chang MW, Rios L, Jillani N, et al. Diurnal transcriptome atlas of a primate
363 across major neural and peripheral tissues. *Science*. 2018 16;359(6381).
- 364 2. Pilonis V, Helfrich-Förster C, Oster H. The role of the circadian clock system in physiology. *Pflügers Arch -*
365 *Eur J Physiol*. 2018 Feb 1;470(2):227–39.
- 366 3. Richards J, Gumz ML. Advances in understanding the peripheral circadian clocks. *FASEB J*. 2012
367 Sep;26(9):3602–13.
- 368 4. Ito C, Tomioka K. Heterogeneity of the Peripheral Circadian Systems in *Drosophila melanogaster*: A
369 Review. *Front Physiol*. 2016;7:8.
- 370 5. Tomioka K, Uryu O, Kamae Y, Umezaki Y, Yoshii T. Peripheral circadian rhythms and their regulatory
371 mechanism in insects and some other arthropods: a review. *J Comp Physiol B, Biochem Syst Environ*
372 *Physiol*. 2012 Aug;182(6):729–40.
- 373 6. Mohawk JA, Green CB, Takahashi JS. Central and peripheral circadian clocks in mammals. *Annu Rev*
374 *Neurosci*. 2012;35:445–62.
- 375 7. Partch CL, Green CB, Takahashi JS. Molecular architecture of the mammalian circadian clock. *Trends Cell*
376 *Biol*. 2014 Feb;24(2):90–9.
- 377 8. Yoo S-H, Yamazaki S, Lowrey PL, Shimomura K, Ko CH, Buhr ED, et al. PERIOD2::LUCIFERASE real-time
378 reporting of circadian dynamics reveals persistent circadian oscillations in mouse peripheral tissues. *Proc*
379 *Natl Acad Sci U S A*. 2004 Apr 13;101(15):5339–46.
- 380 9. Tahara Y, Shibata S. Entrainment of the mouse circadian clock: Effects of stress, exercise, and nutrition.
381 *Free Radical Biology and Medicine*. 2018 May 1;119:129–38.
- 382 10. Bulla M, Oudman T, Bijleveld AI, Piersma T, Kyriacou CP. Marine biorhythms: bridging chronobiology and
383 ecology. *Philos Trans R Soc Lond, B, Biol Sci*. 2017 Nov 19;372(1734).

- 384 11. Last KS, Hendrick VJ. The Clock-Work Worms: Diversity and Function of Clock Expression in Marine
385 Polychaete Worms. In: Annual, Lunar, and Tidal Clocks [Internet]. Springer, Tokyo; 2014 [cited 2018 Jun
386 19]. p. 179–99. Available from: https://link.springer.com/chapter/10.1007/978-4-431-55261-1_10
- 387 12. Tessmar-Raible K, Raible F, Arboleda E. Another place, another timer: Marine species and the rhythms of
388 life. *Bioessays*. 2011 Mar 1;33(3):165–72.
- 389 13. Raible F, Takekata H, Tessmar-Raible K. An Overview of Monthly Rhythms and Clocks. *Front Neurol*
390 [Internet]. 2017 [cited 2018 Dec 31];8. Available from:
391 <https://www.frontiersin.org/articles/10.3389/fneur.2017.00189/full>
- 392 14. Zantke J, Ishikawa-Fujiwara T, Arboleda E, Lohs C, Schipany K, Hallay N, et al. Circadian and Circalunar
393 Clock Interactions in a Marine Annelid. *Cell Reports*. 2013 Oct 17;5(1):99–113.
- 394 15. Kaiser TS, Poehn B, Szkiba D, Preussner M, Sedlazeck FJ, Zrim A, et al. The genomic basis of circadian and
395 circalunar timing adaptations in a midge. *Nature*. 2016 01;540(7631):69–73.
- 396 16. Hauenschild C. Lunar periodicity. *Cold Spring Harb Symp Quant Biol*. 1960;25:491–7.
- 397 17. Schwartz William J., Helm Barbara, Gerkema Menno P. Wild clocks: preface and glossary. *Philosophical*
398 *Transactions of the Royal Society B: Biological Sciences*. 2017 Nov 19;372(1734):20170211.
- 399 18. Connor KM, Gracey AY. Circadian cycles are the dominant transcriptional rhythm in the intertidal mussel
400 *Mytilus californianus*. *Proc Natl Acad Sci USA*. 2011 Sep 20;108(38):16110–5.
- 401 19. Perrigault M, Tran D. Identification of the Molecular Clockwork of the Oyster *Crassostrea gigas*. *PLOS*
402 *ONE*. 2017 Jan 10;12(1):e0169790.
- 403 20. Cook GM, Gruen AE, Morris J, Pankey MS, Senatore A, Katz PS, et al. Sequences of Circadian Clock Proteins
404 in the Nudibranch Molluscs *Hermissenda crassicornis*, *Melibe leonina*, and *Tritonia diomedea*. *Biol Bull*.
405 2018 Jun;234(3):207–18.
- 406 21. Duback VE, Sabrina Pankey M, Thomas RI, Huyck TL, Mbarani IM, Bernier KR, et al. Localization and
407 expression of putative circadian clock transcripts in the brain of the nudibranch *Melibe leonina*. *Comp*
408 *Biochem Physiol, Part A Mol Integr Physiol*. 2018 Sep;223:52–9.
- 409 22. Wilcockson DC, Zhang L, Hastings MH, Kyriacou CP, Webster SG. A novel form of pigment-dispersing
410 hormone in the central nervous system of the intertidal marine isopod, *Eurydice pulchra* (leach). *Journal*
411 *of Comparative Neurology*. 2011;519(3):562–75.
- 412 23. Zhang L, Hastings MH, Green EW, Tauber E, Sladek M, Webster SG, et al. Dissociation of Circadian and
413 Circatidal Timekeeping in the Marine Crustacean *Eurydice pulchra*. *Curr Biol*. 2013 Oct 7;23(19):1863–
414 73.
- 415 24. O'Neill JS, Lee KD, Zhang L, Feeney K, Webster SG, Blades MJ, et al. Metabolic molecular markers of the
416 tidal clock in the marine crustacean *Eurydice pulchra*. *Curr Biol*. 2015 Apr 20;25(8):R326-327.
- 417 25. Hoelters L, O'Grady JF, Webster SG, Wilcockson DC. Characterization, localization and temporal
418 expression of crustacean hyperglycemic hormone (CHH) in the behaviorally rhythmic peracarid
419 crustaceans, *Eurydice pulchra* (Leach) and *Talitrus saltator* (Montagu). *Gen Comp Endocrinol*. 2016
420 01;237:43–52.

- 421 26. Sbragaglia V, Lamanna F, Mat AM, Rotllant G, Joly S, Ketmaier V, et al. Identification, Characterization,
422 and Diel Pattern of Expression of Canonical Clock Genes in *Nephrops norvegicus* (Crustacea: Decapoda)
423 Eyestalk. PLoS ONE. 2015;10(11):e0141893.
- 424 27. Christie AE, Yu A, Roncalli V, Pascual MG, Cieslak MC, Warner AN, et al. Molecular evidence for an intrinsic
425 circadian pacemaker in the cardiac ganglion of the American lobster, *Homarus americanus* - Is diel cycling
426 of heartbeat frequency controlled by a peripheral clock system? Mar Genomics. 2018 Oct;41:19–30.
- 427 28. Takekata H, Matsuura Y, Goto SG, Satoh A, Numata H. RNAi of the circadian clock gene period disrupts
428 the circadian rhythm but not the circatidal rhythm in the mangrove cricket. Biol Lett. 2012 Aug
429 23;8(4):488–91.
- 430 29. Häfker NS, Meyer B, Last KS, Pond DW, Hüppe L, Teschke M. Circadian Clock Involvement in Zooplankton
431 Diel Vertical Migration. Current Biology. 2017 Jul 24;27(14):2194–2201.e3.
- 432 30. Nesbit KT, Christie AE. Identification of the molecular components of a *Tigriopus californicus* (Crustacea,
433 Copepoda) circadian clock. Comp Biochem Physiol Part D Genomics Proteomics. 2014 Dec;12:16–44.
- 434 31. Biscontin A, Wallach T, Sales G, Grudziecki A, Janke L, Sartori E, et al. Functional characterization of the
435 circadian clock in the Antarctic krill, *Euphausia superba*. Scientific Reports. 2017 Dec 18;7(1):17742.
- 436 32. Pittà CD, Biscontin A, Albiero A, Sales G, Millino C, Mazzotta GM, et al. The Antarctic Krill *Euphausia*
437 *superba* Shows Diurnal Cycles of Transcription under Natural Conditions. PLOS ONE. 2013 Jul
438 17;8(7):e68652.
- 439 33. Teschke M, Wendt S, Kawaguchi S, Kramer A, Meyer B. A circadian clock in Antarctic krill: an endogenous
440 timing system governs metabolic output rhythms in the euphausiid species *Euphausia superba*. PLoS ONE.
441 2011;6(10):e26090.
- 442 34. Mazzotta GM, De Pittà C, Benna C, Tosatto SCE, Lanfranchi G, Bertolucci C, et al. A cry from the krill.
443 Chronobiol Int. 2010 May;27(3):425–45.
- 444 35. Kaiser TS, Heckel DG. Genetic Architecture of Local Adaptation in Lunar and Diurnal Emergence Times of
445 the Marine Midge *Clunio marinus* (Chironomidae, Diptera). PLoS One [Internet]. 2012 Feb 22 [cited 2018
446 Jul 23];7(2). Available from: <https://www.ncbi.nlm.nih.gov/pmc/articles/PMC3285202/>
- 447 36. Schenk S, Bannister SC, Sedlazeck FJ, Anrather D, Minh BQ, Bileck A, et al. Combined transcriptome and
448 proteome profiling reveals specific molecular brain signatures for sex, maturation and circalunar clock
449 phase. Elife. 2019 Feb 15;8.
- 450 37. Okano K, Ozawa S, Sato H, Kodachi S, Ito M, Miyadai T, et al. Light- and circadian-controlled genes
451 respond to a broad light spectrum in Puffer Fish-derived Fugu eye cells. Sci Rep. 2017 18;7:46150.
- 452 38. Hur S-P, Takeuchi Y, Esaka Y, Nina W, Park Y-J, Kang H-C, et al. Diurnal expression patterns of
453 neurohypophysial hormone genes in the brain of the threespot wrasse *Halichoeres trimaculatus*. Comp
454 Biochem Physiol, Part A Mol Integr Physiol. 2011 Apr;158(4):490–7.
- 455 39. Mogi M, Uji S, Yokoi H, Suzuki T. Early development of circadian rhythmicity in the suprachiasmatic nuclei
456 and pineal gland of teleost, flounder (*Paralichthys olivaceus*), embryos. Dev Growth Differ. 2015
457 Aug;57(6):444–52.

- 458 40. Park J-G, Park Y-J, Sugama N, Kim S-J, Takemura A. Molecular cloning and daily variations of the Period
459 gene in a reef fish *Siganus guttatus*. *J Comp Physiol A Neuroethol Sens Neural Behav Physiol*. 2007
460 Apr;193(4):403–11.
- 461 41. Rhee J-S, Kim B-M, Lee B-Y, Hwang U-K, Lee YS, Lee J-S. Cloning of circadian rhythmic pathway genes and
462 perturbation of oscillation patterns in endocrine disrupting chemicals (EDCs)-exposed mangrove killifish
463 *Kryptolebias marmoratus*. *Comp Biochem Physiol C Toxicol Pharmacol*. 2014 Aug;164:11–20.
- 464 42. Sánchez JA, Madrid JA, Sánchez-Vázquez FJ. Molecular cloning, tissue distribution, and daily rhythms of
465 expression of *per1* gene in European sea bass (*Dicentrarchus labrax*). *Chronobiol Int*. 2010 Jan;27(1):19–
466 33.
- 467 43. Toda R, Okano K, Takeuchi Y, Yamauchi C, Fukushima M, Takemura A, et al. Hypothalamic expression and
468 moonlight-independent changes of *Cry3* and *Per4* implicate their roles in lunar clock oscillators of the
469 lunar-responsive Goldlined spinefoot. *PLoS ONE*. 2014;9(10):e109119.
- 470 44. Vera LM, Negrini P, Zagatti C, Frigato E, Sánchez-Vázquez FJ, Bertolucci C. Light and feeding entrainment
471 of the molecular circadian clock in a marine teleost (*Sparus aurata*). *Chronobiol Int*. 2013 Jun;30(5):649–
472 61.
- 473 45. Watanabe N, Itoh K, Mogi M, Fujinami Y, Shimizu D, Hashimoto H, et al. Circadian pacemaker in the
474 suprachiasmatic nuclei of teleost fish revealed by rhythmic *period2* expression. *Gen Comp Endocrinol*.
475 2012 Sep 1;178(2):400–7.
- 476 46. Fischer AH, Henrich T, Arendt D. The normal development of *Platynereis dumerilii* (Nereididae, Annelida).
477 *Frontiers in Zoology*. 2010 Dec 30;7:31.
- 478 47. Fischer A, Dorrestein A. The polychaete *Platynereis dumerilii* (Annelida): a laboratory animal with
479 spiral cleavage, lifelong segment proliferation and a mixed benthic/pelagic life cycle. *BioEssays*.
480 2004;26(3):314–25.
- 481 48. Zantke J, Oberlerchner H, Tessmar-Raible K. Circadian and Circalunar Clock Interactions and the Impact
482 of Light in *Platynereis dumerilii*. In: Numata H, Helm B, editors. *Annual, Lunar, and Tidal Clocks: Patterns
483 and Mechanisms of Nature's Enigmatic Rhythms* [Internet]. Tokyo: Springer Japan; 2014 [cited 2018 Dec
484 30]. p. 143–62. Available from: https://doi.org/10.1007/978-4-431-55261-1_8
- 485 49. Tosches MA, Bucher D, Vopalensky P, Arendt D. Melatonin Signaling Controls Circadian Swimming
486 Behavior in Marine Zooplankton. *Cell*. 2014 Sep 25;159(1):46–57.
- 487 50. Fischer A. Über die Chromatophoren und den Farbwechsel bei dem Polychäten *Platynereis dumerilii*.
488 *Zeitschrift für Zellforschung und Mikroskopische Anatomie*. 1964 Mar 1;65(2):290–312.
- 489 51. Röseler I. Untersuchungen über den physiologischen Farbwechsel bei dem Polychaeten *Platynereis*
490 *dumerilii*. *Zool Anz, Suppl-Bd 33, Verh Zool Ges*. 1969;267–73.
- 491 52. Röseler I. Die Rhythmik der Chromatophoren des Polychaeten *Platynereis dumerilii*. *Zeitschrift für*
492 *vergleichende Physiologie*. 1970 Jun 1;70(2):144–74.
- 493 53. Hofmann DK. Regeneration and endocrinology in the polychaete *Platynereis dumerilii* : An experimental
494 and structural study. *Wilehm Roux Arch Dev Biol*. 1976 Mar;180(1):47–71.

- 495 54. Tessmar-Raible K, Arendt D. Emerging systems: between vertebrates and arthropods, the
496 Lophotrochozoa. *Current Opinion in Genetics & Development*. 2003 Aug 1;13(4):331–40.
- 497 55. Hempelmann F. Chromatophoren bei Nereis. *Zeitschr Wiss Zool Abt A*. 1939;152:353–83.
- 498 56. Ayers T, Tsukamoto H, Gühmann M, Veedin Rajan VB, Tessmar-Raible K. A Go-type opsin mediates the
499 shadow reflex in the annelid *Platynereis dumerilii*. *BMC Biol* [Internet]. 2018 Apr 18 [cited 2018 Jul 27];16.
500 Available from: <https://www.ncbi.nlm.nih.gov/pmc/articles/PMC5904973/>
- 501 57. LoopBio. www.loopbio.com. Accessed 17 February 2019.
- 502 58. Veedin Rajan VB, et al. Unpublished.
- 503 59. Hauenschild C. Der hormonale einfluss des Gehirns auf die sexuelle Entwicklung bei dem polychaeten
504 *Platynereis dumerilii*. *General and Comparative Endocrinology*. 1966 Feb 1;6(1):26–73.
- 505 60. Payton L, Perrigault M, Hoede C, Massabuau J-C, Sow M, Huvet A, et al. Remodeling of the cycling
506 transcriptome of the oyster *Crassostrea gigas* by the harmful algae *Alexandrium minutum*. *Scientific*
507 *Reports*. 2017 Jun 14;7(1):3480.
- 508 61. Backfisch B, Rajan VBV, Fischer RM, Lohs C, Arboleda E, Tessmar-Raible K, et al. Stable transgenesis in the
509 marine annelid *Platynereis dumerilii* sheds new light on photoreceptor evolution. *PNAS*. 2013 Jan
510 2;110(1):193–8.
- 511 62. Reppert SM, Weaver DR. Coordination of circadian timing in mammals. *Nature*. 2002 Aug
512 29;418(6901):935–41.
- 513 63. Tosini G, Menaker M. Circadian rhythms in cultured mammalian retina. *Science*. 1996 Apr
514 19;272(5260):419–21.
- 515 64. Balsalobre A, Damiola F, Schibler U. A serum shock induces circadian gene expression in mammalian
516 tissue culture cells. *Cell*. 1998 Jun 12;93(6):929–37.
- 517 65. Dibner C, Schibler U, Albrecht U. The mammalian circadian timing system: organization and coordination
518 of central and peripheral clocks. *Annu Rev Physiol*. 2010;72:517–49.
- 519 66. Schibler U, Ripperger J, Brown SA. Peripheral circadian oscillators in mammals: time and food. *J Biol*
520 *Rhythms*. 2003 Jun;18(3):250–60.
- 521 67. Fingerman M. Persistent Daily and Tidal Rhythms of Color Change in *Callinectes sapidus*. *Biological*
522 *Bulletin*. 1955;109(2):255–64.
- 523 68. Fingerman M, Rao KR, Ring G. Restoration of a Rhythm of Melanophoric Pigment Dispersion in
524 Eyestalkless Fiddler Crabs, *Uca Pugilator* (Bosc), At a Low Temperature 1). *Crustaceana*. 1969 Jan
525 1;17(1):97–105.
- 526 69. Fingerman M, Yamamoto Y. Daily Rhythm of Melanophoric Pigment Migration in Eyestalkless Fiddler
527 Crabs, *Uca Pugilator* (Bosc). *Crustaceana*. 1967 Jan 1;12(3):303–19.
- 528 70. Darnell MZ. Ecological physiology of the circadian pigmentation rhythm in the fiddler crab *Uca panacea*.
529 *Journal of Experimental Marine Biology and Ecology*. 2012 Sep 1;426–427:39–47.

- 530 71. Stevens M, Rong CP, Todd PA. Colour change and camouflage in the horned ghost crab *Ocypode*
531 *ceratophthalmus*. *Biological Journal of the Linnean Society*. 2013 Jun 1;109(2):257–70.
- 532 72. Stevens M. Color Change, Phenotypic Plasticity, and Camouflage. *Frontiers in Ecology and Evolution*.
533 2016;4:51.
- 534 73. Shahidi R, Williams EA, Conzelmann M, Asadulina A, Veraszto C, Jasek S, et al. A serial multiplex
535 immunogold labeling method for identifying peptidergic neurons in connectomes. *eLife*. 2015 Dec
536 15;4:e11147.
- 537 74. Nery LE, Da Silva MA, Castrucci AM. Possible role of non-classical chromatophorotropins on the
538 regulation of the crustacean erythrophore. *J Exp Zool*. 1999 Nov 1;284(6):711–6.
- 539 75. Schmid B, Helfrich-Förster C, Yoshii T. A new ImageJ plug-in “ActogramJ” for chronobiological analyses. *J*
540 *Biol Rhythms*. 2011 Oct;26(5):464–7.

541

542 **Figure Legends**

543 **Fig. 1.** Relative transcript levels of *bmal*, *period* and *tr-cry* in (A) heads under LD conditions, (B) trunks under
544 LD conditions and (C) trunks in DD conditions on intact animals (*i.e.* not decapitated). ZT= Zeitgeber Time and
545 CT= Circadian Time. p-value estimated on a single factor ANOVA with n=6, 15 and 11 for A, B and C respectively
546 (alpha= 0.05). Error bars denote SEM.

547 **Fig. 2.** Relative transcript levels of (A) *bmal*, (B) *period* (C) and *tr-cry* in trunks of decapitated animals placed
548 under (A) LD and (B) DD conditions for three days. ZT= Zeitgeber Time. CT= Circadian Time. p-value estimated
549 on a single factor ANOVA with n=6 on each treatment (alpha= 0.05). Error bars denote SEM.

550 **Fig. 3.** Relative transcript levels of *bmal*, *period* and *tr-cry* in trunks of decapitated animals placed under
551 inverted LD conditions for seven days with either white, blue or red color (for light spectra and intensity see
552 Additional file 2: Figure S2). ZT= Zeitgeber Time. CT= Circadian Time. p-value estimated on a single factor
553 ANOVA with (alpha= 0.05). Error bars denote SEM.

554 **Fig. 4.** (A) Sexually immature *P. dumerilii* adult under standard light microscopy. (B) Same individual as in (A),
555 now autofluorescent under 488 nm light and a FITC filter, with chromatophores clearly visible as bright green
556 circles (prominent green autofluorescence of the jaws can also be see in the anterior end). (C) Average

557 chromatophore size based on autofluorescence (see materials and methods) of the same group of individuals
558 followed over a 24h period (n=15) under standard LD conditions. Pairwise student's t-Tests (preceded by F-
559 Tests) were performed comparing each of the ZT hours. Individual averages from ZT2 to ZT5 and ZT14 to ZT23
560 were statistically similar within them but not between them in all permutations possible (alpha=0.05). Error
561 bars denote SEM.

562 **Fig. 5.** Fluorescent microscopy images of chromatophore size difference between (A) ZT12 and (B) ZT14 under
563 standard LD conditions. (C) Average chromatophore size at ZT/CT 12 and ZT/CT 14 before and after five days
564 under DD conditions (n=4). (D) Average chromatophore size at ZT/CT 12 and ZT/CT 14 over seven consecutive
565 days. Dashed line indicates decapitation and placement in DD conditions. Red arrow indicates re-placement
566 under LD conditions (n=6) (see Additional file 3: Figure S3 for individual replicas). (E) Average chromatophore
567 size, over a 24h period, of individuals before and five days after decapitation (n=10). (F) Average
568 chromatophore size at ZT12 and ZT14 of individuals before and five days after decapitation and placement on
569 an inverted LD cycle (n=6). For (C)(D)(F), pairwise student's t-Tests (preceded by F-Tests) were performed
570 comparing ZT/CT 2 and ZT/CT 14 at each sampling day. For (E), p-value was estimated on a single factor ANOVA.
571 Error bars denote SEM and alpha= 0.05 in all cases.

572 **Fig. 6.**

573 Individual locomotor activity of intact (n=20) and headless (n=30) worms under 16h light and 8h dark (LD)
574 conditions followed by three days of constant darkness (DD). (A,C) Average double plotted actograms of intact
575 (A) and headless (C) worms. Black bar indicates night hours whereas yellow bar indicates day hours during LD
576 conditions. Decapitation of headless worms was performed at ZT14 one day before recording (=LD0) . (B,D)
577 Average distance moved of intact (B) and headless worms (D) during day and nighttime, as well as during
578 different time periods of constant darkness (i.e. CT4-CT16 for subjective day, and CT16-CT4 for an extended
579 subjective night). The subjective night period (CT16-CT0) was extended to CT4 because under DD conditions
580 activity levels cycle with a ca. 25h \pm 0.22 period (mean \pm SEM, see Additional file 4: Figure S4 B), and therefore

581 activity during DD1-3 darkness is expected to run into the early phase of the subjective day. For day and night
582 time activity, only data from LD3 and and LD4 were pooled, because during the first two days after head
583 removal worms hardly moved. Bars indicate mean \pm SEM. p-values were calculated using repeated measures
584 ANOVA followed by Sidak's multiple comparison test with ****p < 0.0001, **p<0.01, *p<0.05

585

586

587 **Additional Material**

588 File name: Additional file 1

589 File format: PDF

590 Title of data: Figure S1

591 Description of data: Relative transcript levels of (A) *timeless*, (B) *pdp1* and (C) *clock* in trunks of intact animals
592 (*i.e.* not decapitated) under standard LD conditions (n= 5 to 8 per ZT point); and of (D) *bmal*, (E) *period* and (F)
593 *tr-cry* on the last 5-7 segments of the body (black line) or the adjacent 5-7 segments towards the anterior part
594 of the animal (red line) (n=3 in all cases). ZT= Zeitgeber Time. p-value estimated on a single factor ANOVA
595 (α = 0.05). Error bars denote SEM.

596

597 File name: Additional file 2

598 File format: PDF

599 Title of data: Figure S2

600 Description of data: (A) Spectra and intensity of light used for re-entrainment of animals (see Figs. 2-3 in the
601 main text). (B) White light spectrum used in the locomotor activity assay.

602

603 File name: Additional file 3

604 File format: PDF

605 Title of data: Figure S3

606 Description of data: Individual replicas of animals used on Fig. 5C, showing chromatophore size at ZT/CT 12
607 and ZT/CT 14 over seven consecutive days. Dashed line indicates decapitation and placement in DD conditions.
608 Red arrow indicates re-placement under LD conditions (n=6). ZT= Zeitgeber Time and CT= Circadian Time.

609

610 File name: Additional file 4

611 File format: PDF

612 Title of data: Figure S4

613

614 (A) Individual locomotor activity of intact worms under 16h light and 8h dark (LD) conditions followed by three
615 days of constant darkness (DD) depicted in individual double plotted actograms. Black bar indicates night hours
616 whereas yellow bar indicates day hours during LD conditions. Decapitation of headless worms was performed
617 at ZT14 one day before recording (=LD0). (B) Lomb-Scargle periodogram analysis of activity data recorded
618 under DD1-3 reveals a circadian free running period of $25.0\text{h} \pm 0.22\text{ h}$ (n=10, mean \pm SEM). Only periods that
619 had a power value >20 were considered (power values of >10 were already classified to be significantly
620 rhythmic ($p<0.05$) by the Lomb-Scargle analyses, but we used a more stringent cut-off to reduce the probability
621 of detecting false-positive periods). Out of the 20 worms tested only the first 10 worms depicted in (A) show
622 power values >20 , and therefore only these were considered to calculate the mean period length.

623

624 File name: Additional file 5

625 File format: PDF

626 Title of data: Figure S5

627 Description of data: Individual locomotor activity of headless worms under 16h light and 8h dark (LD)

628 conditions followed by three days of constant darkness (DD) depicted in individual double plotted actograms.

629 Black bar indicates night hours whereas yellow bar indicates day hours during LD conditions. Decapitation of

630 headless worms was performed at ZT14 one day before recording (=LD0)



HeadsLD



TrunksLD



TrunksDD

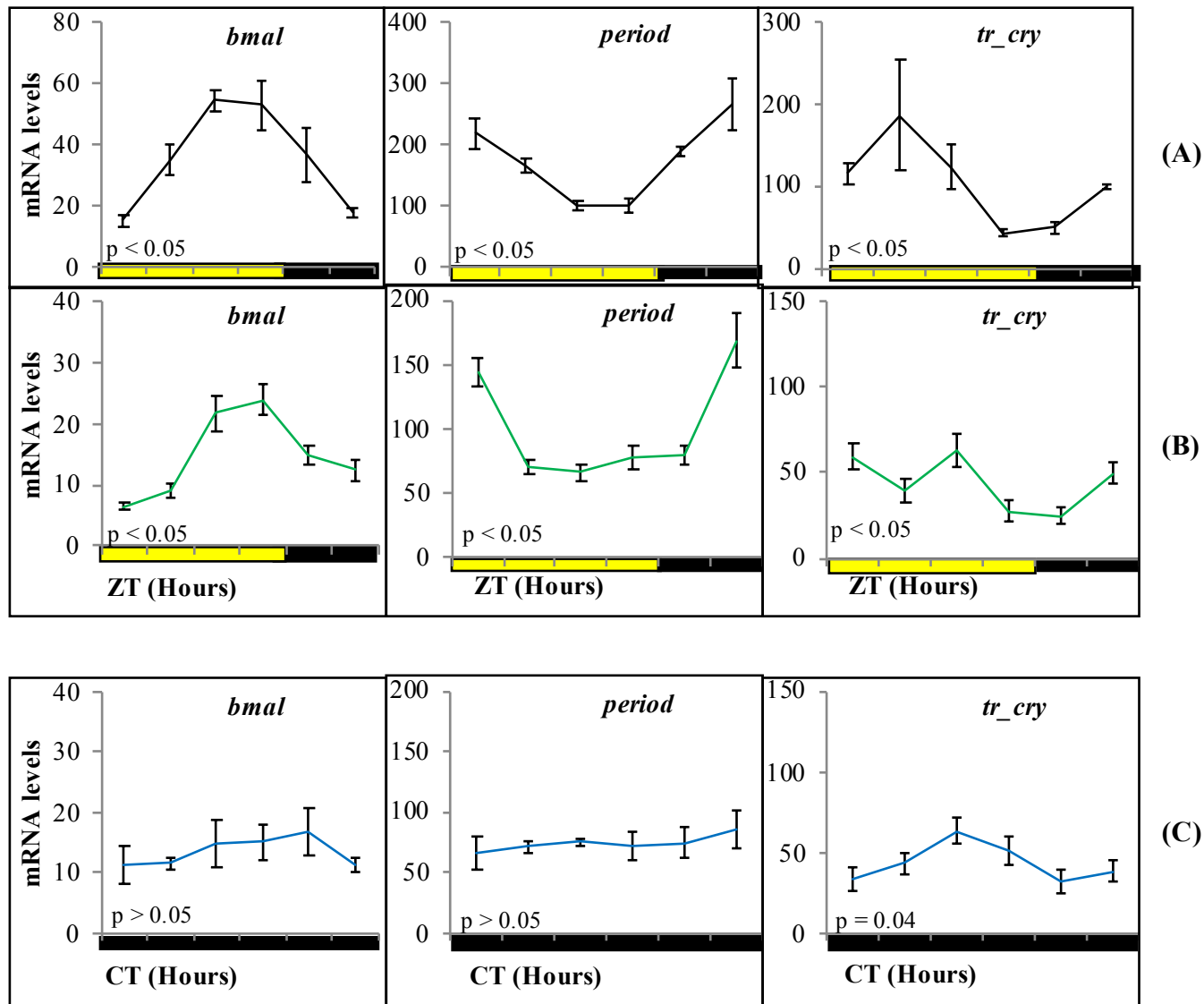


Figure 1

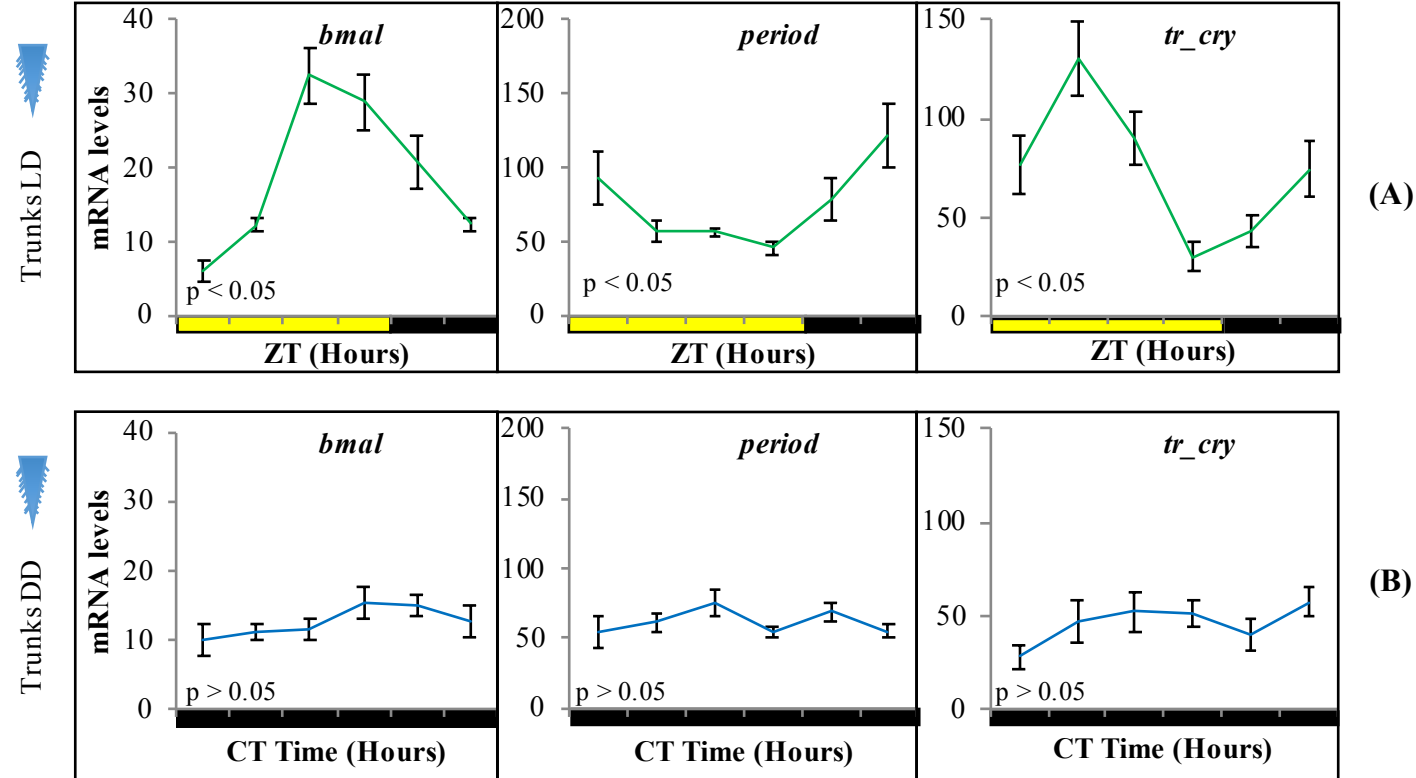


Figure 2

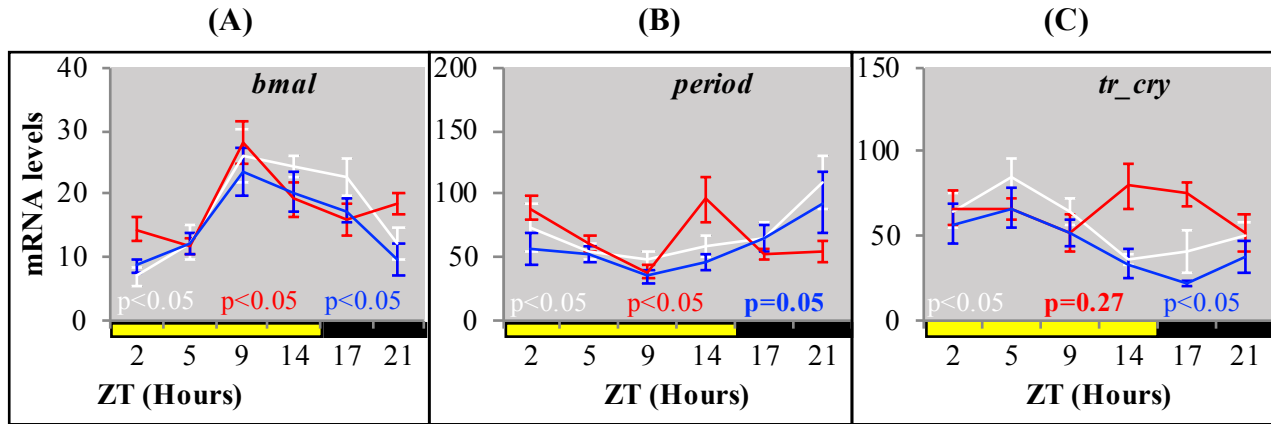
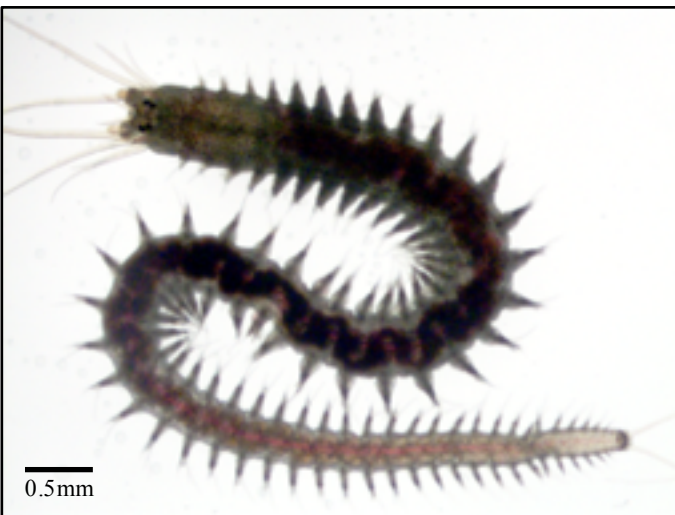
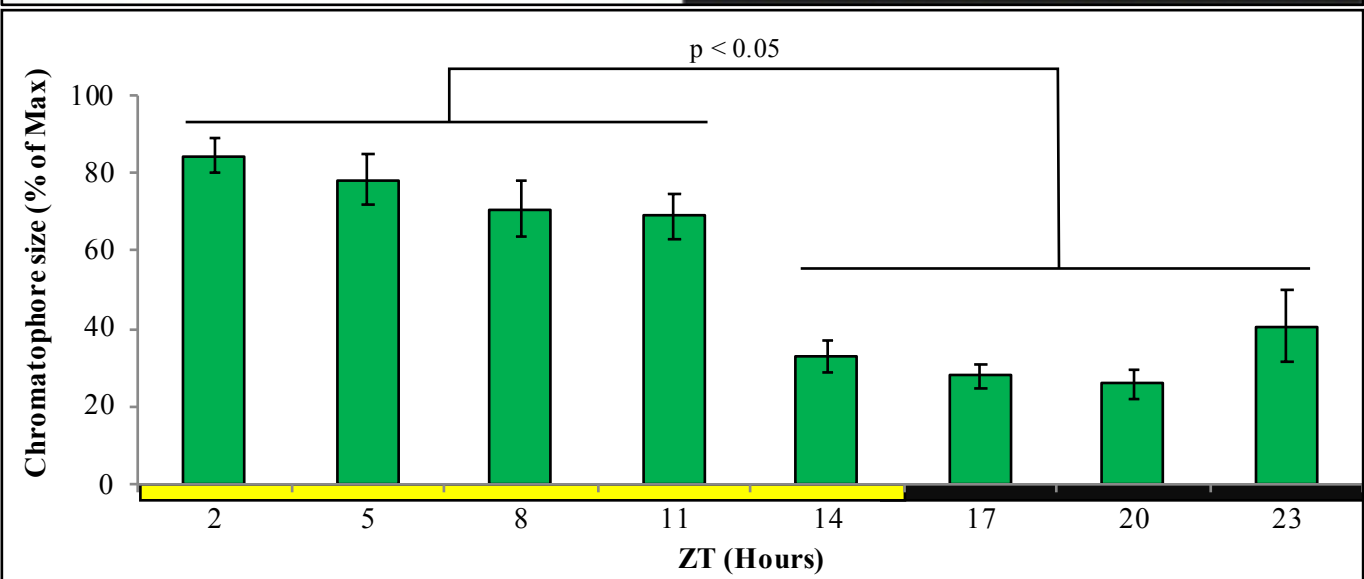
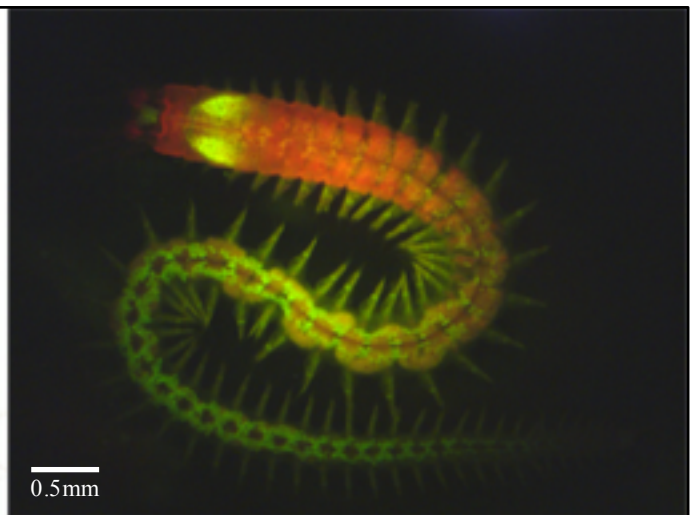
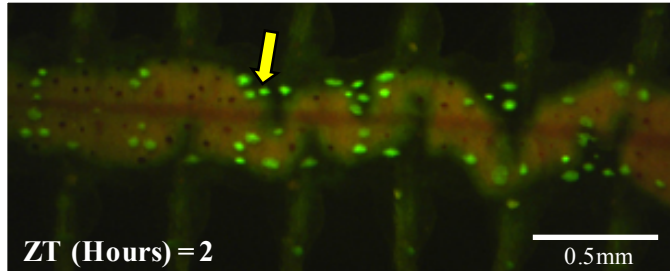


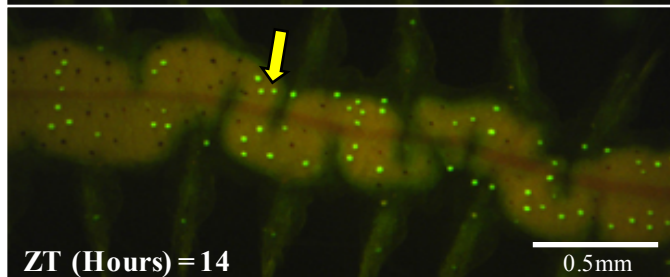
Figure 3

(A)**(B)****Figure 4**

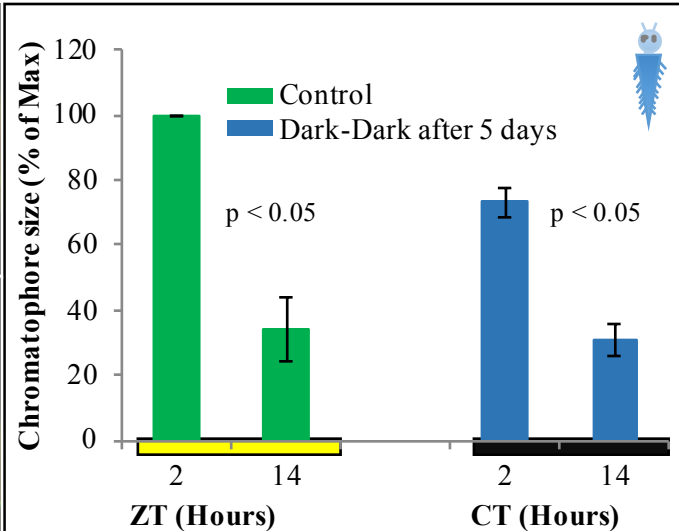
(A)



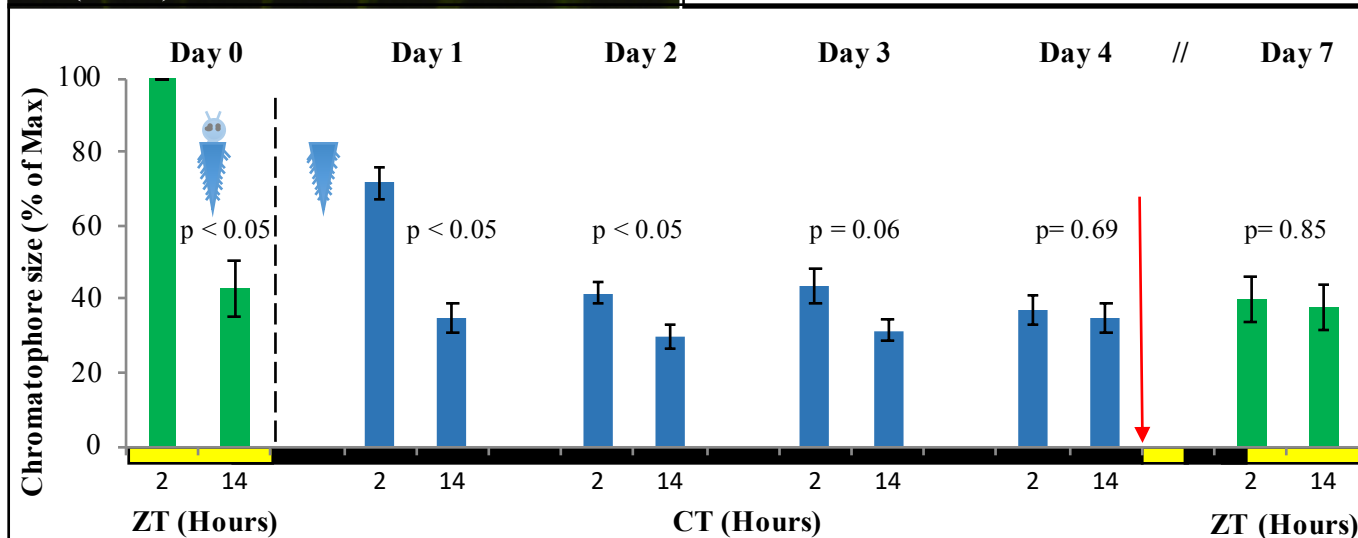
(B)



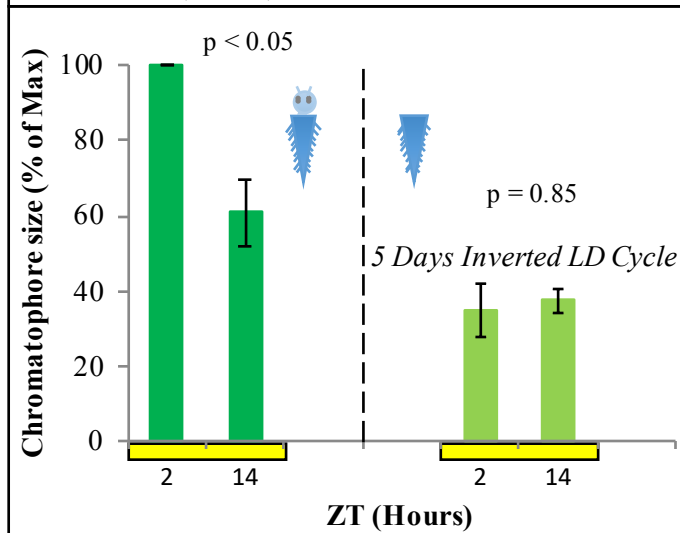
(C)



(D)



(E)



(F)

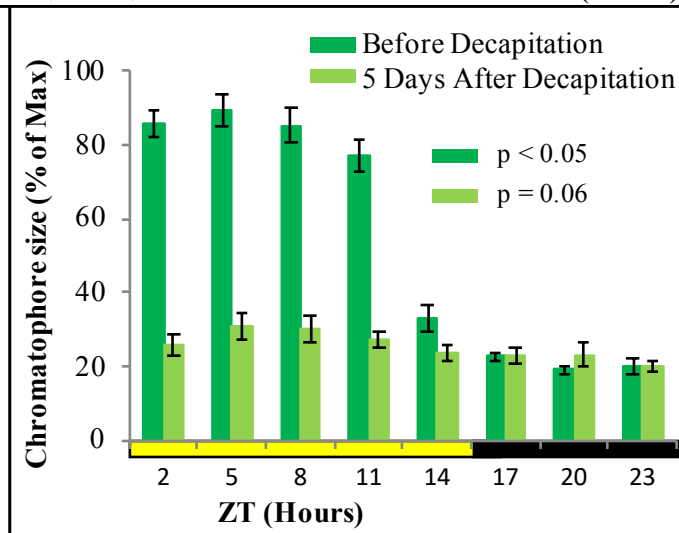


Figure 5

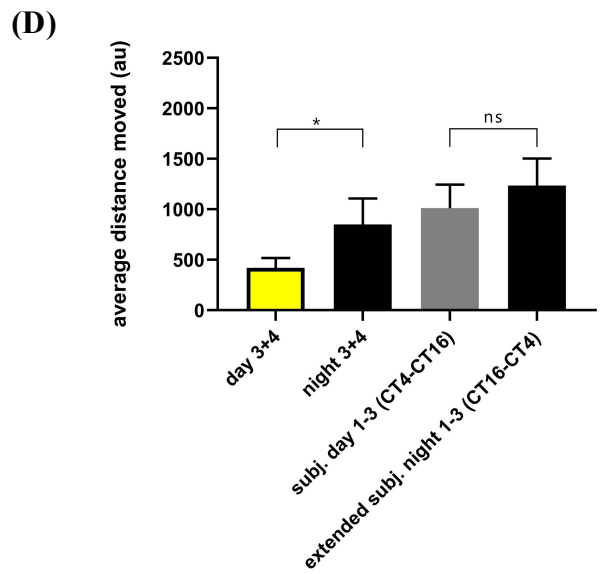
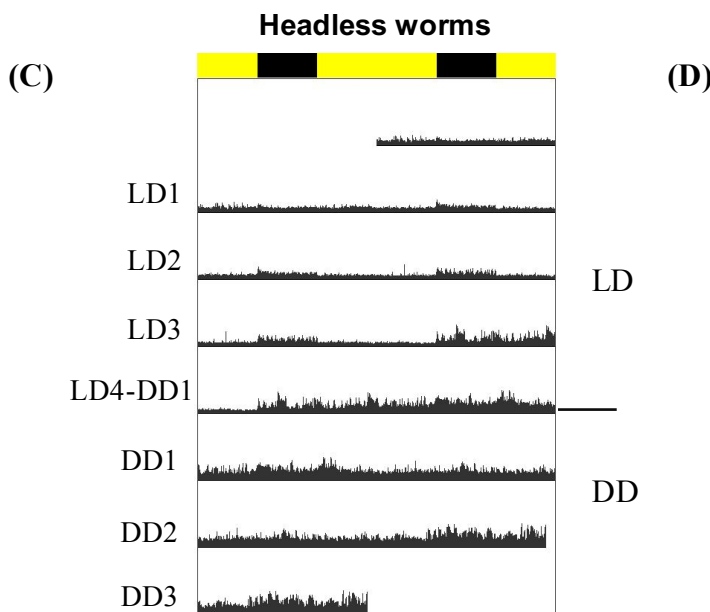
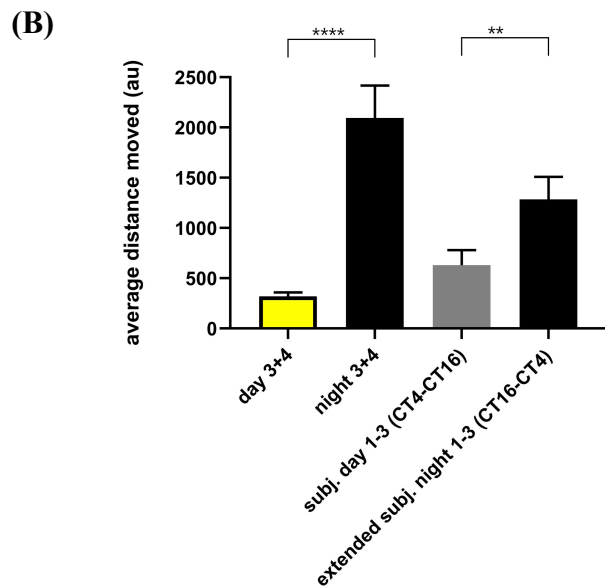
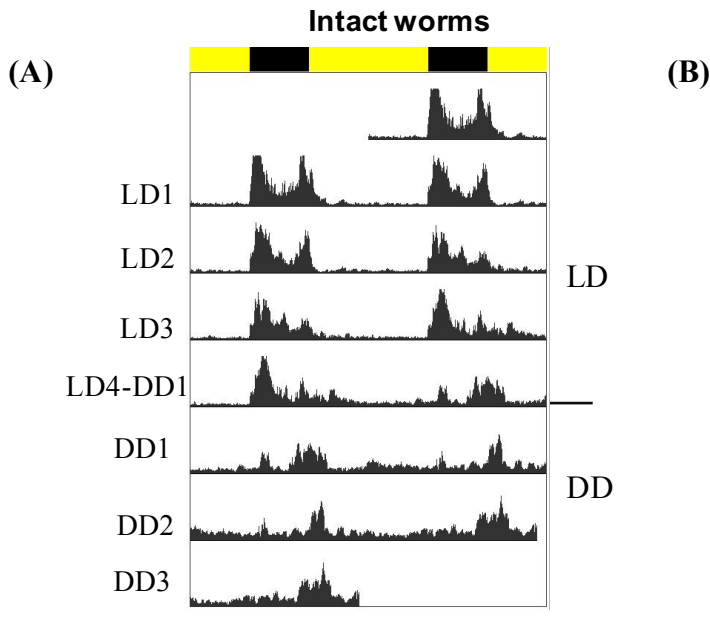
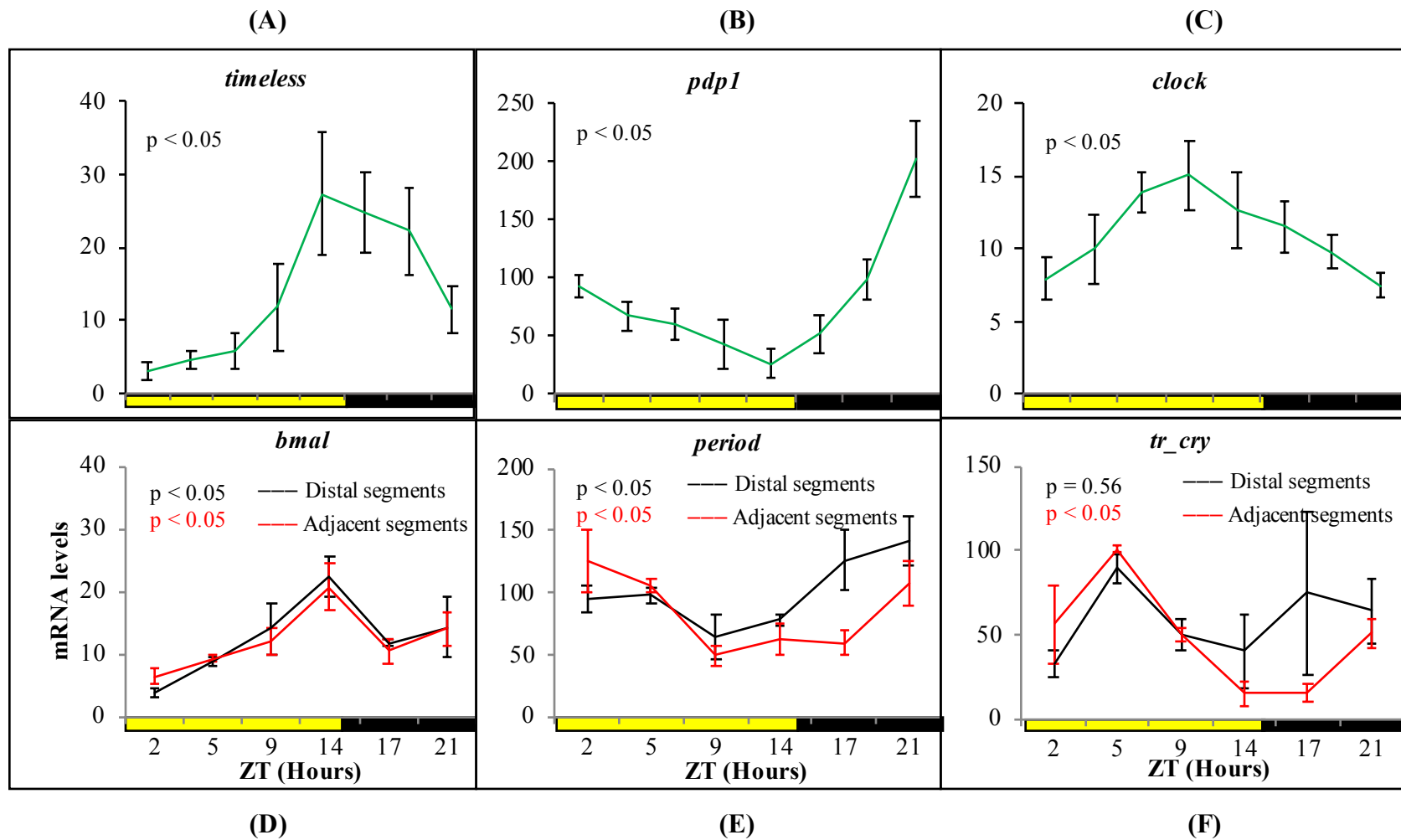
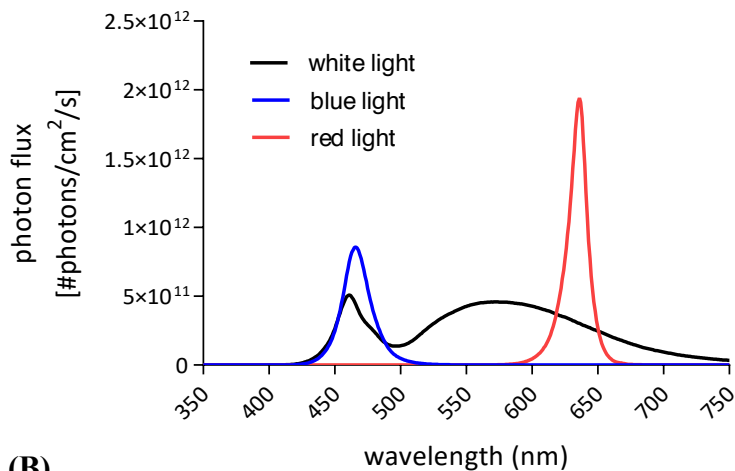
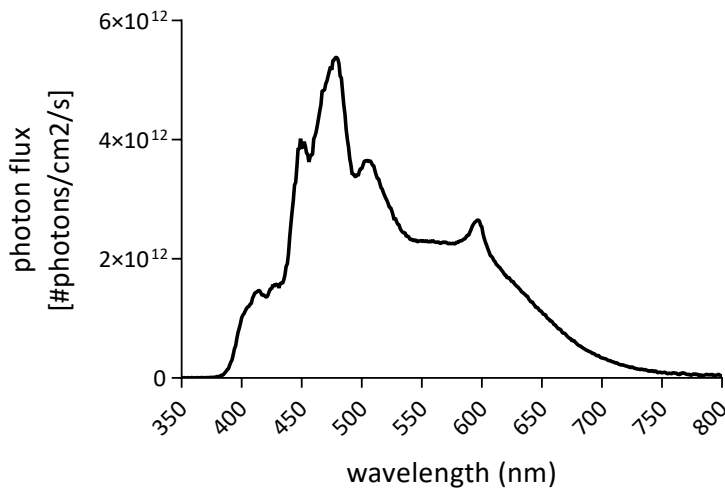


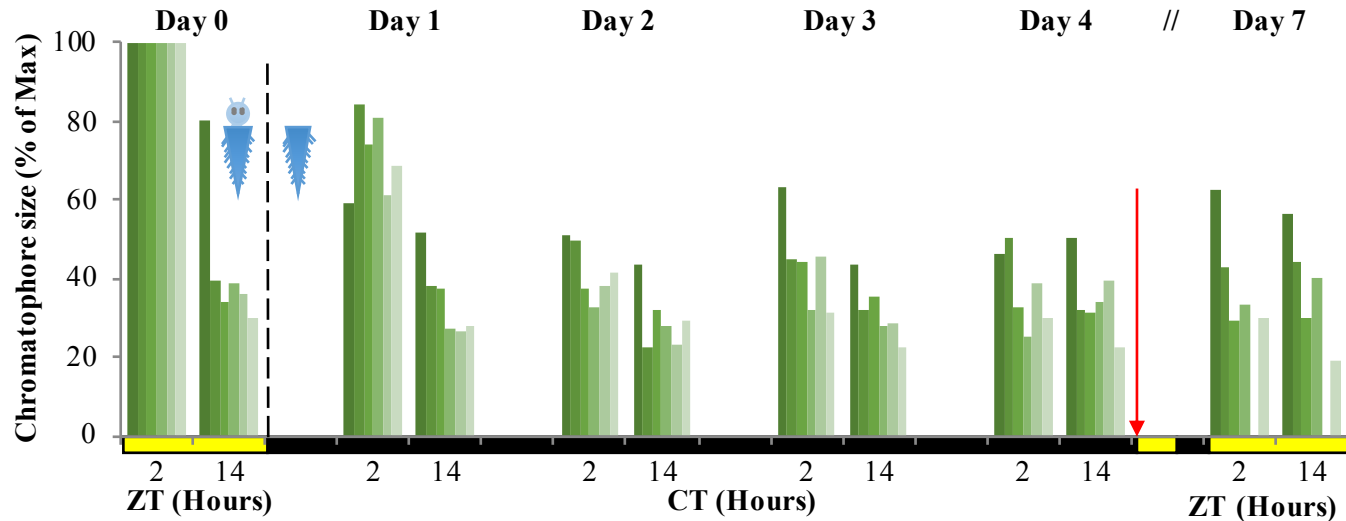
Figure 6

TrunksLD

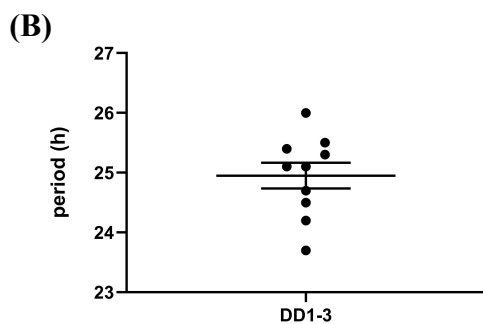
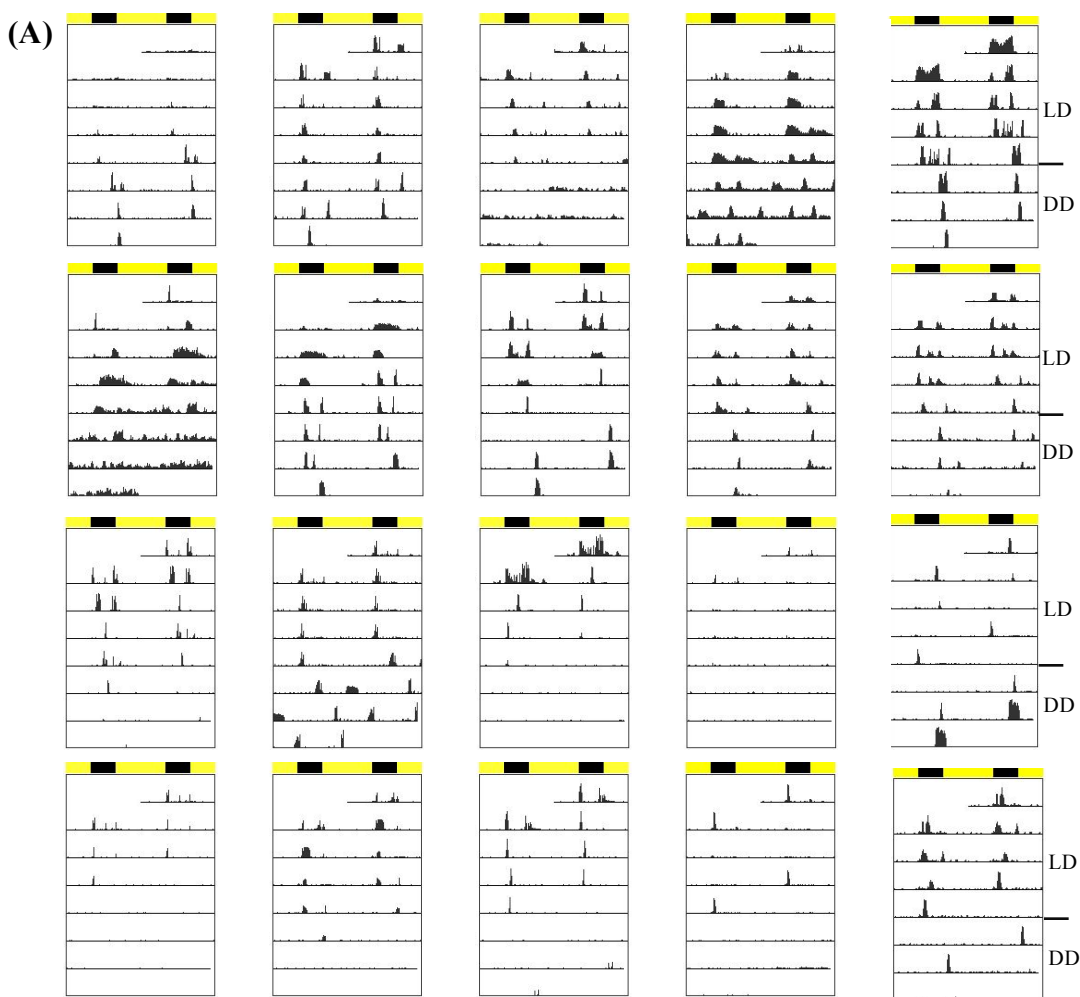
TrunksLD

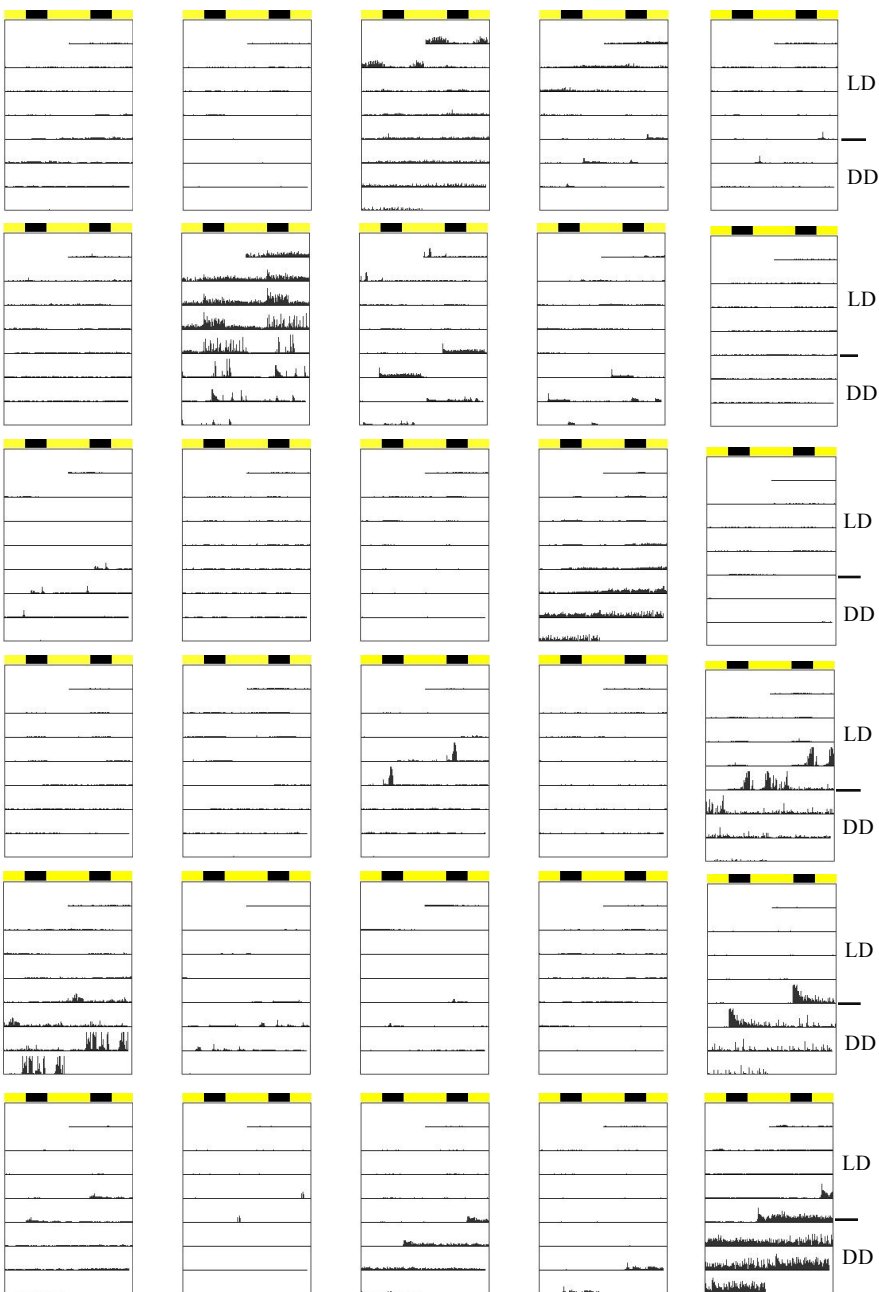


(A)**(B)**



Additional file 3: Figure S3





Additional file 5: Figure S5